Electronic Supplementary Material (ESI) for Dalton Transactions.

Supporting Information

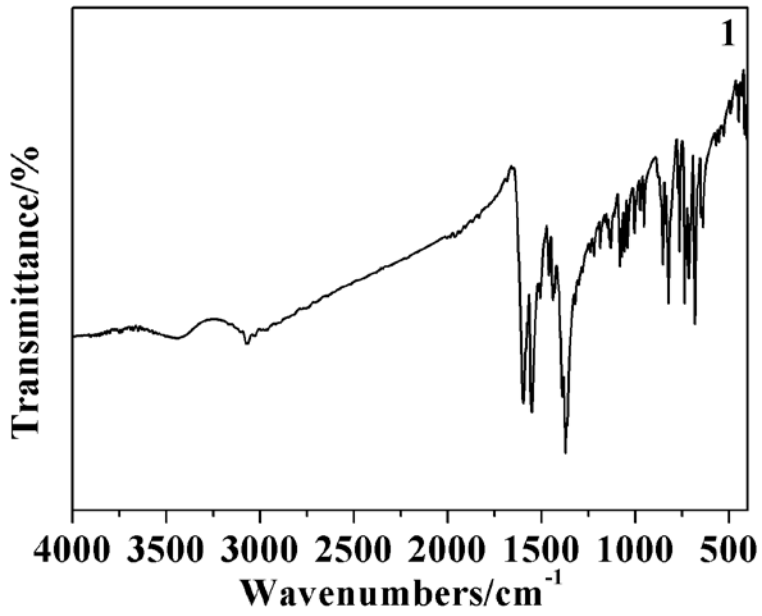

Figure S1a. IR spectrum of complex **1**.

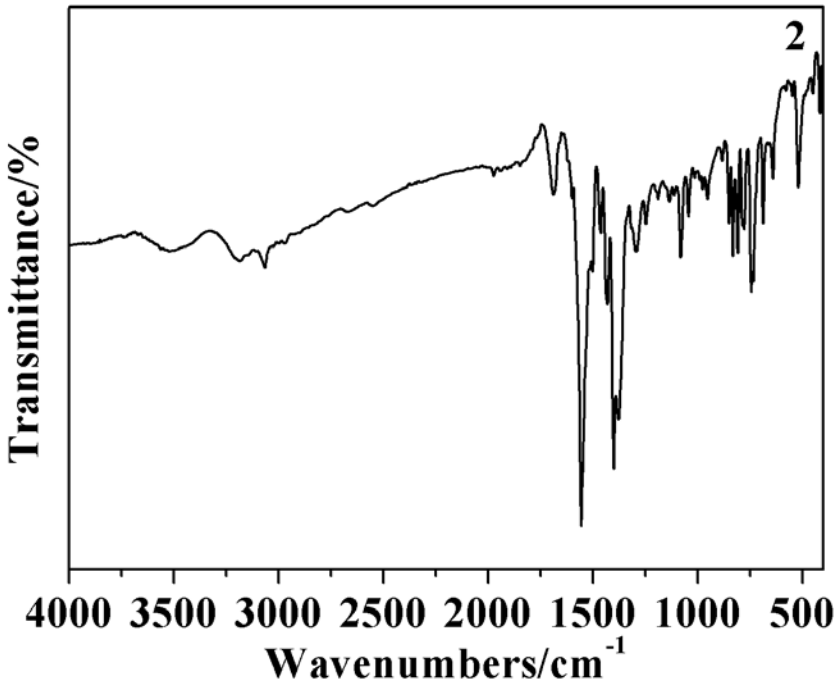

Figure S1b IR spectrum of complex **2.**

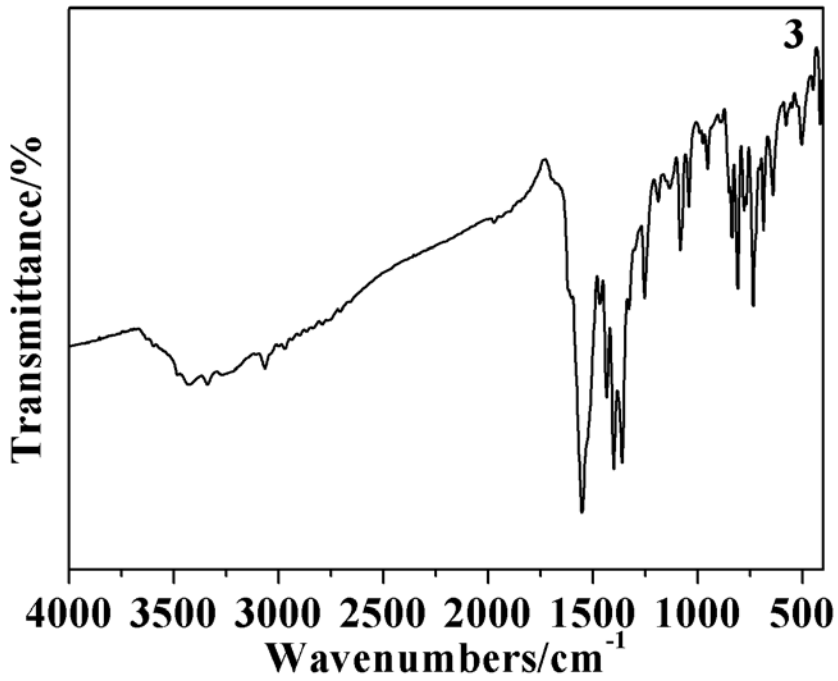

Figure S1c. IR spectrum of complex **3**.

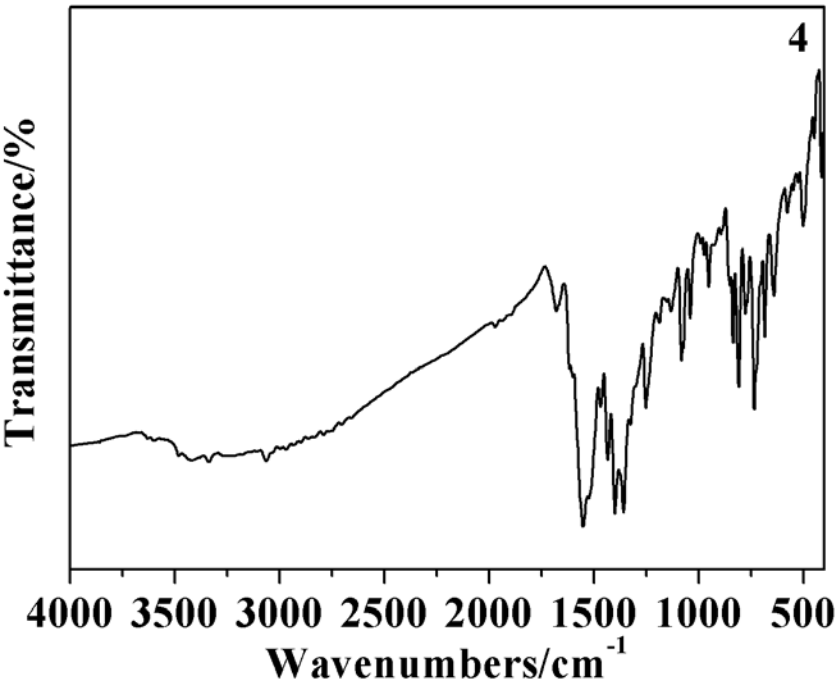

Figure S1d. IR spectrum of complex **4**.

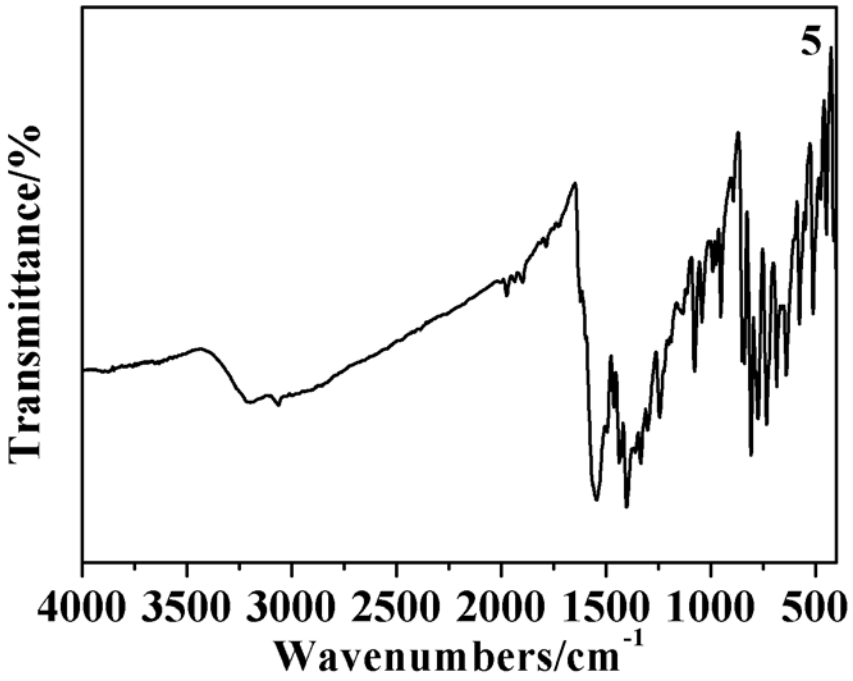

Figure S1e. IR spectrum of complex **5**.

Structure of [Pb(2-NCP)(L_3)$_{0.5}$]$_n$ (**4**) It is similar to **3** that the asymmetric unit of the complex **4** also contains of one crystallographically independent Pb^{2+} ion, one 2-NCP^- ligand and half a L_3^{2-} ligand. As shown in Figure S2, Pb^{2+} is also in a seven-coordinated environment, completed by two nitrogen atoms (N1, N2) belonging to the same 2-NCP^- ligand and five oxygen atoms ($O1^{\#3}$, $O1^{\#4}$, $O2^{\#3}$, O3, O4, symmetry code: #3 x+1/2, -y+1/2, z+1/2; #4 -x, -y, -z+1) from two 2-NCP^- ligands and one L_3^{2-} ligand. The Pb-O and Pb-N lengths are in the range of 2.380(2)-2.755(3) Å and 2.500(3)-2.595(3) Å, respectively. These distances are comparable to those in the previously reported Pb^{2+} complexes.[7,8]

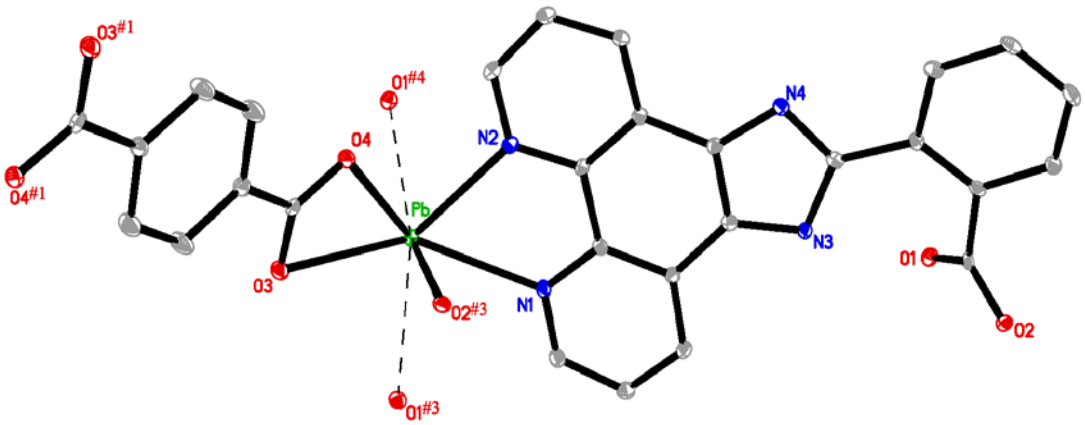

Figure S2. ORTEP view of **4** showing the local coordination environments of Pb^{2+} atoms with hydrogen atoms omitted for clarity (30% probability displacement ellipsoids). Symmetry codes: #1 -x, -y, -z+2; #3 x+1/2, -y+1/2, z+1/2; #4 -x, -y, -z+1.

Structure of $[Pb_2(2\text{-NCP})_2(L_4)]_n$ (5). It is similar to **3** that the asymmetric unit of the complex **5** also contains of one crystallographically independent Pb^{2+} ion, one 2-NCP^- ligand and half a L_4^{2-} ligand. As shown in Figure S3, Pb^{2+} is also in a seven-coordinated environment, supplied by five oxygen atoms ($O1^{\#3}$, $O2^{\#3}$, O3, O4, $O1^{\#4}$, symmetry code: #3 *x*-1/2, -*y*+1/2, *z*-1/2; #4 -*x*+2, -*y*, -*z*+2) from two different 2-NCP^- and one L_4^{2-} ligands, two nitrogen atoms (N1, N2) from one 2-NCP^- ligand. It is noted that there are three oxygen atoms ($O1^{\#3}$, $O1^{\#4}$, O4) coordinated with center metal by weak interaction. The average Pb-O and Pb-N distances are 2.421(3) Å and 2.550(4) Å, respectively, which are quite similar to the normal Pb-O and Pb-N distances.[7,8]

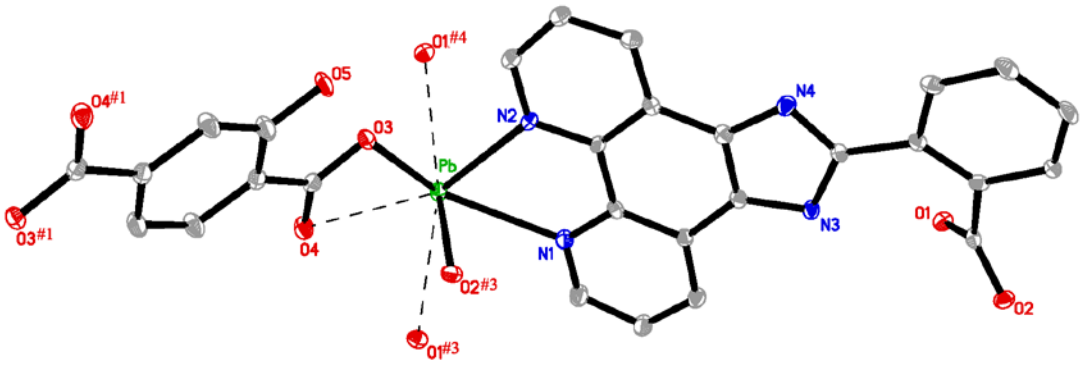

Figure S3. ORTEP view of **5** showing the local coordination environments of Pb^{2+} atoms with hydrogen atoms omitted for clarity (30% probability displacement ellipsoids). Symmetry codes: #1 -*x*+2, -*y*, -*z*+1; #3 *x*-1/2, -*y*+1/2, *z*-1/2; #4 -*x*+2, -*y*, -*z*+2.

Photocatalytic degradation of different organic dyes. The amine functionalized 3D structure for

3 showed superior photocatalytic activity to that of other complexes. Therefore, we use it as photocatalyst to further study the degradation efficiency of other organic dyes such as methyl orange (MO), rhodamine-6G (RD 6G), rhodamine-B(RD), congo red (CR), and crystal violet (CV), the results are shown in Figure S4a, and the characteristic absorption peak of different organic dyes significantly decreases as the photocatalytic reaction proceeds as show in Figure S4c. It can be seen that approximately 58.2% of CV, 39.4% of MO, 71.6% of CR, 19.7% of RD 6G and 44.3% of RD have been decomposed after 280 min of irradiation for **3**, respectively. These results indicated that the complex is more active for the decomposition of MB under visible light irradiation. The dots of the experimental data and the fitted least-square line show the order of different organic pollutions degradation rate for as-prepared photocatalyst **3** was CR (4.24×10^{-3} min^{-1}) > CV (2.82×10^{-3} min^{-1}) > RD (2.09×10^{-3} min^{-1}) > MO (1.54×10^{-3} min^{-1}) > RD 6G (0.06×10^{-3} min^{-1}) > blank (2.15×10^{-3} min^{-1}, 2.12×10^{-3} min^{-1}, 2.71×10^{-3} min^{-1}, 3.05×10^{-3} min^{-1}, 2.68×10^{-3} min^{-1}, respectively), and the resuls are shown in Figure S4b.

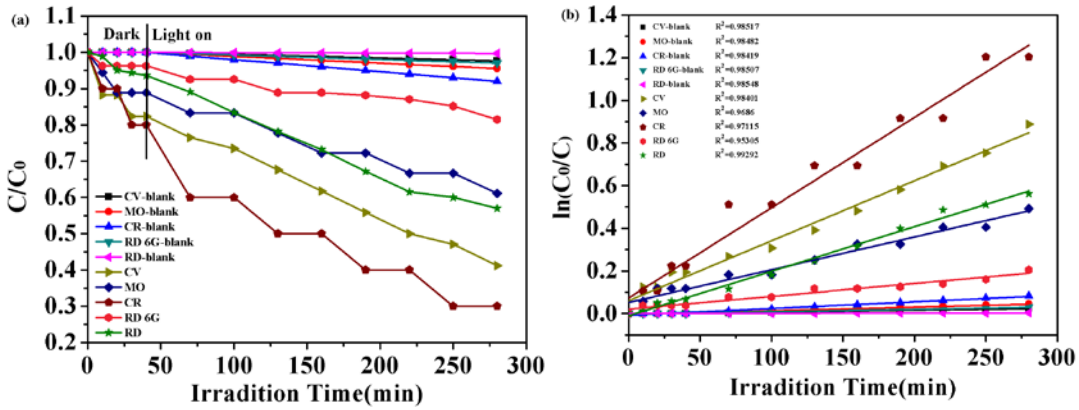

Figure S4. (a) The photocatalytic decomposition rate of CR, CV, RD, MO and RD 6G solution under visible-light irradiation with the photocatalytic activities of **3**; (b) The pseudo-first-order plot for the photodegradation of CR, CV, RD, MO and RD 6G in the presence of **3** under visible-light irradiation. The dots and line represent the experimental data and the fitted least-square line, respectively.

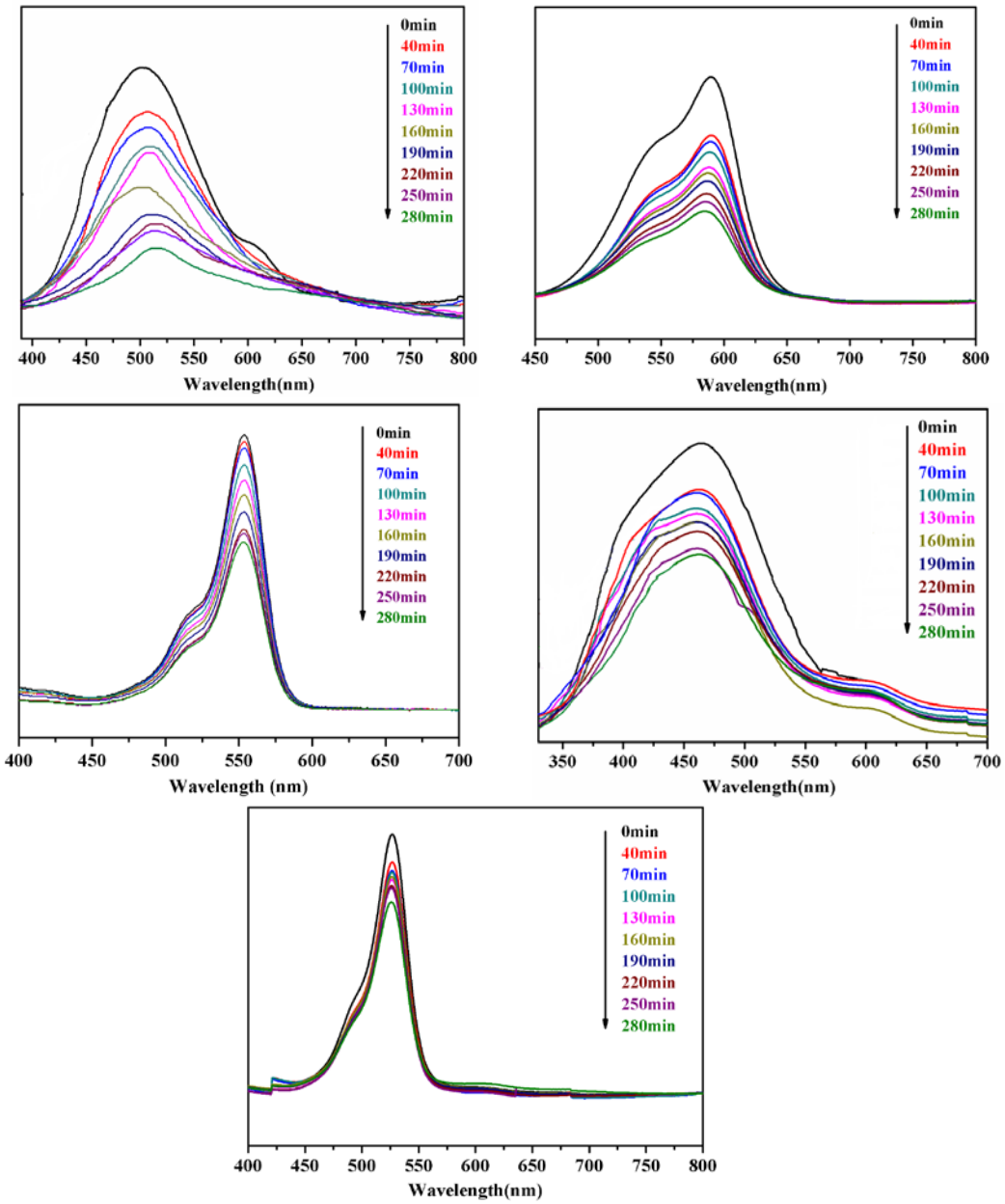

Figure S4c. The UV-vis absorption spectra of the CR, CV, RD, MO and RD 6G solution during the decomposition reaction under visible light irradiation in the presence of photocatalyts **3**, respectively.